

This is the accepted manuscript made available via CHORUS. The article has been published as:

Population Genetics in Compressible Flows

Simone Pigolotti, Roberto Benzi, Mogens H. Jensen, and David R. Nelson

Phys. Rev. Lett. **108**, 128102 — Published 23 March 2012

DOI: [10.1103/PhysRevLett.108.128102](https://doi.org/10.1103/PhysRevLett.108.128102)

Population genetics in compressible flows

Simone Pigolotti^{1,2}, Roberto Benzi³, Mogens H. Jensen¹ and David R. Nelson⁴

¹*The Niels Bohr Institut, Blegdamsvej 17, DK-2100 Copenhagen, Denmark.* ²*Dept. de Fisica i Eng. Nuclear, Universitat Politecnica de Catalunya Edif. GAIA, Rambla Sant Nebridi s/n, 08222 Terrassa, Barcelona, Spain.* ³*Dipartimento di Fisica, Universita' di Roma "Tor Vergata" and INFN, via della Ricerca Scientifica 1, 00133 Roma, Italy.* ⁴*Lyman Laboratory of Physics, Harvard University, Cambridge, MA 02138, USA*

(Dated: today)

We study competition between two biological species advected by a compressible velocity field. Individuals are treated as discrete Lagrangian particles that reproduce or die in a density-dependent fashion. In the absence of a velocity field and fitness advantage, number fluctuations lead to a coarsening dynamics typical of the stochastic Fisher equation. We investigate three examples of compressible advecting fields: a shell model of turbulence, a sinusoidal velocity field and a linear velocity sink. In all cases, advection leads to a striking drop in the fixation time, as well as a large reduction in the global carrying capacity. We find localization on convergence zones, and very rapid extinction compared to well-mixed populations. For a linear velocity sink, one finds a bimodal distribution of fixation times. The long-lived states in this case are demixed configurations with a single interface, whose location depends on the fitness advantage.

PACS numbers: 87.23.Cc, 47.27.E-

Challenging problems arise when spatial migrations of species are combined with population genetics. The population dynamics of a single species expanding into new territory was first studied in the pioneering works of Fisher, Kolmogorov, Petrovsky and Piscounov (FKPP) [1–3]. Later, Kimura and Weiss studied individual-based counterparts of the FKPP equation [4], revealing the important role of number fluctuations. In particular, stochasticity is inevitable at a frontier, where the population size is small and the discrete nature of the individuals becomes essential. Depending on the parameter values, fluctuations can produce radical changes with respect to the deterministic predictions [3, 5]. If $f(x, t)$ is the population fraction of, say, a mutant species and $1 - f(x, t)$ that of the wild type, the stochastic FKPP equation reads in one dimension [6]:

$$\partial_t f(x, t) = D \partial_x^2 f + s f(1 - f) + \sqrt{D_g f(1 - f)} \xi(x, t) \quad (1)$$

where D is the spatial diffusion constant, D_g is the genetic diffusion constant (inversely proportional to the local population size), s is the genetic advantage of the mutant and $\xi = \xi(x, t)$ is a Gaussian noise, delta-correlated in time and space that must be interpreted using Ito calculus [6, 7]. In the neutral case ($s = 0$), number fluctuations induce a striking effect in the population dynamics, namely segregation of the two species. In 1D, segregation can be studied by looking at the dynamics of genetic interfaces between the $f = 0$ and $f = 1$ states of Eq. 1, which behave as coalescing random walkers. This effect is confirmed experimentally in the linear inoculation experiments on neutral variants of fluorescently labelled bacteria illustrated in Fig. (1a) [23].

However, many species, from the distant past [8] up to the present, have competed in liquid environments, such

as lakes, rivers and oceans. Interesting new phenomena arise when population dynamics is coupled to hydrodynamic flows [9], especially in presence of turbulence [10]. Moreover, recent observations demonstrated how advection can have a crucial role in determining the outcome of biological competition. For example, a recent study [11] demonstrated how the invasion of a european variant of a crab species in the eastern North American coast was determined by the direction of transport of larvae by sea currents rather than any selective advantage. Further, satellite observations of chlorophyll concentrations have identified long lived, segregated patches of marine microorganisms off the eastern coast of South America [12], where the tangential velocity field obtained from satellite altimetry seems to have a determining role in segregating the domains of different species.

When modeling competition in the ocean, it is often appropriate to consider a *compressible* velocity field, both because of inertial effects [13] associated with fairly large microorganisms (diameter 5-500 μ m), and because photosynthetic bacteria and plankton often control their buoyancy to stay close to the ocean surface [14]. In the latter case, the coarse-grained velocity field advecting the microorganisms will contain a compressible component to account for downwellings [15]. Gyrotaxis, the mechanism by which swimming microorganisms try to maintain their preferential direction [16], can also be thought as an effective compressible flow acting on the organisms.

Recent works studied the dynamics of a single population in the presence of a compressible turbulent velocity field in one and two dimensions [17, 18]. Here, the interplay between turbulent dynamics and population growth leads to quasilocation on convergence zones and a reduction in the *carrying capacity*, defined as the limit on the

total population size imposed by competition.

Our interest is to study the effect of advection on the dynamics of two distinct populations. Due to competition and stochasticity, interactions between two populations usually drive one of them to extinction. The average time of this event (*fixation time*, in population genetics jargon) is a quantity of great biological interest since it determines the amount of genetic and ecological diversity that the system can sustain. Studying competition in a hydrodynamics context, where both a compressible velocity field and stochasticity due to finite population sizes are present, calls for a nontrivial generalization of Eq. (1). One complication is that, because of compressibility, the sum of the concentrations of the two species is no longer invariant during the dynamics. Thus, we must clarify the definition of $f(x, t)$, the fraction of one particular species. A biologically important issue arises from overshooting: the density $f(x, t)$ can exceed unity near velocity sinks, resulting in an unphysical imaginary noise amplitude in Eq. (1). This anomaly arises because Eq. (1) assumes a fixed total concentration of individuals, so that if $f(x, t)$ is the concentration of one species, the other must have a concentration exactly equal to $1 - f(x, t)$.

In this Letter, we overcome these problems by introducing a new off-lattice particle model designed to explore how compressible velocity fields affect biological competition. We consider two different organisms, A and B , which advect and diffuse in space while undergoing duplication (i.e. cell division) and density-dependent annihilation (death). Specifically, we implement the following stochastic reactions: each particle of species $i = A, B$ duplicates with rate μ_i and annihilates with rate $\bar{\mu}_i \hat{n}_i$, where \hat{n}_i is the number of neighboring particles (of both types) in an interaction range δ . Let N be the total number of organisms that can be accommodated in the unit interval with total density $c_A + c_B = 1$. To reduce the number of parameters, we fix $\delta = 1/N$ as the average particle spacing in the absence of flow. Further, we set $\bar{\mu}_A = \bar{\mu}_B = \mu_B = \mu$, but take $\mu_A = \mu(1 + s)$ to allow for a selective advantage (faster reproduction rate) of species A . The particle model is simulated with a second order Adams-Bashforth scheme for the particle positions. At each time step, the probabilities of particles of duplicating or being annihilated by competition are computed from the rates defined above; the list of particles is then stochastically updated. In the case of duplication, a daughter particle is created at the same coordinate as the mother. We will start by analyzing in depth the neutral case $s = 0$ and consider the effect of $s > 0$ in the end of the Letter. In one dimension and with these choices of parameters, our macroscopic coupled equations for the densities $c_A(x, t)$ and $c_B(x, t)$ of individuals of type A and B in an advecting field $v(x, t)$

read

$$\begin{aligned} \partial_t c_A &= -\partial_x(v c_A) + D \partial_x^2 c_A + \mu c_A(1 + s - c_A - c_B) + \sigma_A \xi \\ \partial_t c_B &= -\partial_x(v c_B) + D \partial_x^2 c_B + \mu c_B(1 - c_A - c_B) + \sigma_B \xi' \end{aligned} \quad (2)$$

with $\sigma_A = \sqrt{\mu c_A(1 + s + c_A + c_B)/N}$ and $\sigma_B = \sqrt{\mu c_B(1 + c_A + c_B)/N}$. $\xi(x, t)$ and $\xi'(x, t)$ are independent delta-correlated noise sources with an Ito-calculus interpretation as in Eq. (1).

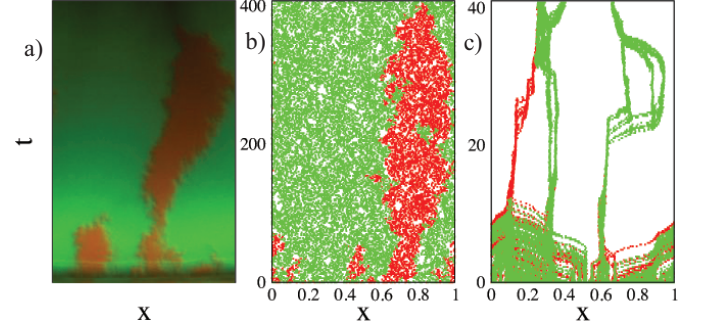


FIG. 1: (a) Experimental range expansion of the two neutral *E. coli* strains used in Ref. [23], but grown about one day longer (D. Nelson, unpublished). The black bar at the bottom is due a small crack in the agar substrate. (b) Space-time plot of the off-lattice particle model with no advecting velocity field. A realization characterized by a pattern similar to the experimental one has been selected for illustrative purposes. (c) Particle model with a compressible turbulent velocity field. Simulations are run until fixation (disappearance of one of the two species); note the reduced carrying capacity and the much faster fixation time in (c). Parameters: $N = 10^3$, $D = 10^{-4}$, $\mu = 1$. Parameters of the shell model are as in [17].

The above equations follow from a microscopic master equation via the Kramers-Moyal method [20], at this order equivalent to Van Kampen inverse system size expansion [21]. Multi-species versions of the FKPP equations have been already considered in Refs [22], but not in the presence of an advecting field or number fluctuations. Although $s = 0$ may seem nongeneric in the context of dynamical systems theory, this is a case of particular interest in population genetics, where it corresponds to the neutral theory of Kimura [4].

Simulations of the particle model with $v = s = 0$ result in a dynamics similar to the one observed in experiments, as shown in Fig.(1b). In this simple limit, our model can be considered as a grand canonical generalization of Eq (1), where the total density of individuals $c_A + c_B$ is now allowed to fluctuate around an average value 1. Details of the numerical implementation and the role of density fluctuations are presented in [20]. Hereafter, we fix the following parameters: $N = 10^3$, $D = 10^{-4}$, $\mu = 1$ and $L = 1$ where L is a one dimensional domain endowed with periodic boundary conditions. With these parameters, the fixation time τ_f would be $\sim 10^4$ for the

one dimensional FKPP equation, and $\sim 10^3$ for the well-mixed case.

Introducing a compressible velocity field $v(x, t)$, as shown in Fig.(1c), leads to radically different dynamics. Individuals tend to concentrate at long-lived sinks in the velocity field. Further, extinction is enhanced and the total number of individuals $n(t)$ present at time t is on average smaller than N . In order to study how a velocity field changes τ_f , we first analyze two different velocity fields: The first is a velocity field $v(x, t)$ generated by a shell model of compressible turbulence [17, 19], reproducing the power spectrum of high Reynolds number turbulence with forcing intensity F [20]. The second is a static sine wave, $v(x) = F \sin(2\pi x)$, representing a simpler case in which only one Fourier mode is present, and thus a single sink, in the advecting field. In both cases, periodic boundary conditions on the unit interval are implemented.

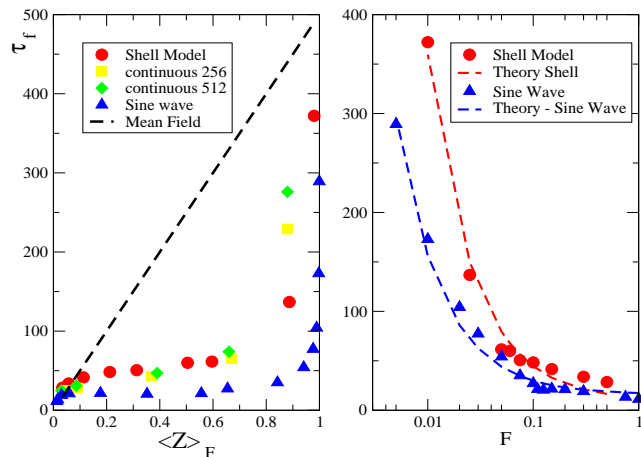


FIG. 2: Average fixation time τ_f for neutral competitions in compressible turbulence and sine wave advection, as a function of (left) the reduced carrying capacity $\langle Z \rangle_F$ and (right) forcing intensity F (small $\langle Z \rangle_F$ in the left panel corresponds to large forcing in the right panel). (left) Red circles and blue triangles are particle simulations. Other symbols denote simulations of the continuum equations with different resolutions on the unit interval. The black dashed line is the mean field prediction, $\tau_f = N\langle Z \rangle_F/2$. In (right), particle simulations are compared with the theoretical prediction $\tau_f = \tau_0 + c/F$ (dashed lines), with fitted parameters $\tau_0 = 9.5$, $c = 3.5$ for the shell model and $\tau_0 = 16$, $c = 1.4$ for the sine wave.

Fig.(2) shows the average fixation time τ_f for $s = 0$ in the first two cases, while varying the intensity F of advection. In the left panel, we plot the fixation times as a function of the time-averaged reduced carrying capacity $\langle Z \rangle_F$, where $Z(t) = n(t)/N$ is the carrying capacity reduction, i.e. the ratio between the actual number of particles and the average number of particles N observed in absence of the velocity field. Plotting vs. $\langle Z \rangle_F$ allows comparisons with the mean field prediction, $\tau_f = 2N\langle Z \rangle_F/\mu$, valid for well mixed systems (black

dashed line) [6]. For the shell model, we include simulations of the macroscopic equations (2) with different resolutions (256 and 512 lattice sites on the unit interval), obtaining always similar results for τ_f vs. $\langle Z \rangle_F$.

In all cases, the presence of a spatially varying velocity field leads to a dramatic reduction of τ_f , compared to mean field theory. The fixation time drops abruptly as soon as $\langle Z \rangle < 1$, even for very small F . Simulations suggest a singular limit of zero intensity ($F \sim 0$) of the velocity field (and consequently $\langle Z \rangle \rightarrow 1$ in Fig. 2), as we discuss later.

To understand these observations note that global fixation represents the coalescence of all the interfaces between the species, like those shown in Fig. (1a) and (1b). While in the case $s = v = 0$ the interfaces perform a random walk [6], here they are also advected by the velocity field. In particular, the average position x of one interface, neglecting diffusion and number fluctuations, evolves according to $\dot{x} = v(x, t)$. The fixation time is determined by the time needed for all interfaces to reach the center of a sink and annihilate. Because periodic boundary conditions are imposed, the number of interfaces is always even, so all eventually annihilate via pairwise collision. Upon expanding the velocity field around a sink position x_0 , $v(x) = k(x_0 - x)$, we find a characteristic time $\sim k^{-1}$. The fixation time can be then estimated as $\tau_f = \tau_0 + ck^{-1}$, where τ_0 is the typical time to reach fixation at large strain rate k and c is a dimensionless constant of order unity. This phenomenological theory describes well the data of Fig. 2, right panel (dashed lines), where in the turbulent case we take the forcing F as a proxy for k ($k = 2\pi F$ for the sine wave and $k = \sqrt{\langle (\nabla v)^2 \rangle} \propto F$ for turbulence). For an *odd* number of interfaces, new phenomena could arise, as the fixation time can become extremely long when only one interface is left.

We study this possibility by introducing a converging linear velocity field, $v(x) = -kx$ with open boundary conditions, so that the number of interfaces is no longer topologically constrained to be even. At large k (small $\langle Z \rangle_k$), the fixation time is comparable to the mean field prediction. However, as the forcing decreases, it becomes much *larger* than the mean field prediction (Fig. 3a, dashed line). In this regime, the fixation time probability distribution is bimodal (Fig. 3a, inset): roughly half of the realizations have a short fixation time (faster than mean field), while the other half maintain coexistence for an extended period. The space-time evolution of these configurations in Fig. 3b reveals that the two mutant species are *demixed*, with one dominant on the left and one on the right of the sink. This configuration corresponds to a stable stationary solution of the deterministic version of Eqs (2) with $s = 0$. We expect this demixed solution to have a lifetime (inaccessible in our numerical simulations) which grows exponentially with N [7, 21]. Correspondingly, the average total heterozygosity $\langle H(t) \rangle$,

defined as the probability of two random individuals to be of different type [6], decays exponentially for very large k (consistent with mean field theory [6]), but tends to a constant, non-zero value for small values of k (Fig 3c).

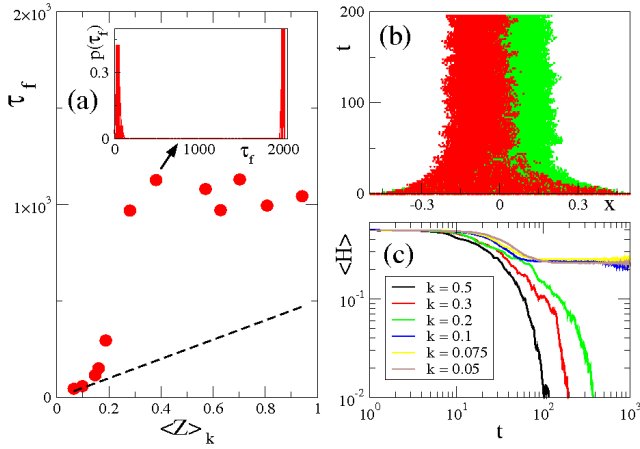


FIG. 3: (a) Average fixation time τ_f in the presence of a linear converging flow $v = -kx$, as a function of the reduced carrying capacity $\langle Z \rangle_k$. Inset on left shows the distribution of fixation times in the case $k = 0.075$ and $\langle Z \rangle_k \approx 0.38$; the right peak represents all realizations with fixation times $t > 2000$. (b) Space-time plot of a realization with a very long fixation time. (c) Average heterozygosity as a function of time for different values of k .

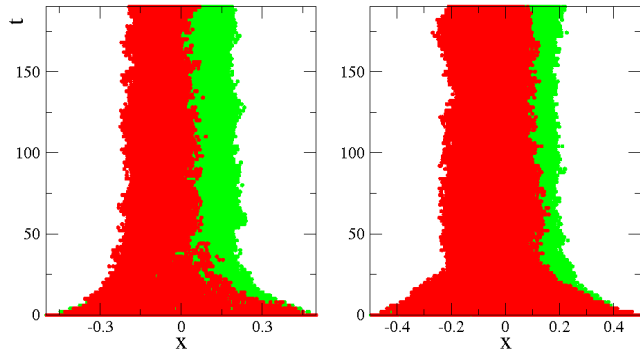


FIG. 4: Coexistence of two species advected by a linear sink $k = 0.075$, (left) species are neutral as in Fig. 3, (right) Red reproduces 30% faster. Notice the shift in the position of the interface.

Introducing a selective advantage combined with hydrodynamic flows leads to an even richer scenario. In traditional population genetics, a more fit species (with a selective advantage μs) expands into the territory of a less fit one with a velocity $v = 2\sqrt{D\mu s}$ (also known as Fisher velocity [1], see [5] for an extension to the strong noise limit). In this case, such velocity can be offset by advection. This is shown in fig. 4, where the neutral case of Fig. 3 is compared with a simulation in which red particles reproduce 30% faster ($s = 0.3$). Even with

such a large selective advantage, a genetic interface is still present. We can estimate the rightward shift in the interface position away from zero as $\delta x = k^{-1}2\sqrt{D\mu s}$, by equating the outward Fisher genetic wave velocity $v_g = 2\sqrt{D\mu s}$ [1] with the inward advection velocity at distance δx from the origin. Because Fisher wave velocities are typically much smaller than velocities of marine currents [11], the outcome of competition in aquatic systems will often be determined by the properties of the flow rather than the species growth rates.

To conclude, we have introduced a new model of off-lattice particle dynamics to study how compressible advection affects Darwinian competition. Compressible flows lead to a remarkable new scenario, with the fixation time now largely determined by how interfaces among species collapse into the sinks of the velocity field, rather than by diffusive annihilation. Our phenomenological theory suggests a significant effect even for very weak compressible fields. Compressible advection becomes irrelevant for the fixation time only when the time to drift into the sinks (of order $t \sim k^{-1}$) is much larger than the diffusion time (of order $L^2 D^{-1}$, where L is a typical linear size of the population). An obvious application of the model is the study of compressible flows in higher space dimensions, including flows relevant to biological oceanography of photosynthetic organisms near the water surface. Recent advances in experimental techniques could also lead to tests of the one dimensional results. Motility of bacteria has been studied in microstructures of diameter comparable or even smaller to that of the organisms [24]. In this setting, a compressible flow could be created by pumping liquid nutrient into the two ends of the tube and extracting it from the center via a semipermeable membrane. Another possibility could be to study floating microorganisms [14, 25] and exploit the compressible effects caused by the vertical component of a convecting velocity field [15].

We are grateful to F. Toschi and P. Perlekar for interesting discussions. Work by SP and MHJ was supported by the Danish National Research Foundation through the Center for Models of Life. Support for DRN was provided by the National Science Foundation in part through Grant No. DMR-1005289 and by the Harvard Materials Research Science and Engineering Center through NSF Grant No. DMR-0820484.

-
- [1] R. A. Fisher, *Ann. Eugenics* **7**, 353-369 (1937).
 - [2] A. Kolmogorov, N. Petrovsky, and N. Piscounov, *Moscow Univ. Math. Bull.* **1**, 1-25 (1937).
 - [3] W. van Saarloos, *Phys. Rep.* **386**, 29-222 (2003).
 - [4] M. Kimura and G. H. Weiss, *Genetics* **49**, 561-576 (1964); J. F. Crow and M. Kimura *An Introduction to Population Genetics*, Blackburn Press, Caldwell, NJ (2009).
 - [5] O. Hallatschek and K. Korolev, *Phys. Rev. Lett.* **103**,

- 108103 (2009), and references therein.
- [6] For a recent review, see K. Korolev et al. *Rev. Mod. Phys.* **82**, 1691-1718 (2010).
 - [7] C. Gardiner *Handbook of Stochastic Methods: for Physics, Chemistry and the Natural Sciences*, Springer Series in Synergetics (2004).
 - [8] B. A. Whitton and M. Potts *The Ecology of Cyanobacteria: Their Diversity in Time and Space* eds. Kluwer, Dordrecht, Netherlands (2000).
 - [9] T. Tel et al., *Physics Reports* **413**, 91196 (2005).
 - [10] W. J. McKiver and Z. Neufeld, *Phys. Rev. E* **79**, 061902 1-8 (2009).
 - [11] J. M. Pringle, A. M. H. Blakeslee, J. E. Byers and J. Roman, *Proc. Natl. Acad. Sci.* **108**, 15288-15293 (2011).
 - [12] F. D'Ovidio et al., *Proc. Natl. Acad. Sci.* **107**, 18366-18370 (2010).
 - [13] J. Bec, *Phys. Fluids* **15**, L81-L84 (2003).
 - [14] A. P. Martin, *Progr. Ocean.* **57**, 125-174 (2003).
 - [15] J. R. Cressman et al., *Europhys. Lett.* **66**, 219-225 (2004); G. Boffetta et al., *Phys. Rev. Lett.* **93**, 134501 (2004).
 - [16] W. M. Durham, E. Climent, R. Stocker, *Phys. Rev. Lett.* **106**, 238102 (2011); C. Torney, Z. Neufeld, *Phys. Rev. Lett.* **99**, 078101 (2007).
 - [17] R. Benzi, D. R. Nelson *Physica D* **238** 2003-2015 (2009).
 - [18] P. Perlekar et al., *Phys. Rev. Lett.* **105**, 144501 (2010).
 - [19] M. H. Jensen et al., *Phys. Rev. A* **43**, 798-805 (1991) ; T. Bohr et al., *Dynamical Systems Approach to Turbulence* Cambridge University Press, Cambridge (1998).
 - [20] Supplementary Material are available online.
 - [21] N. G. van Kampen *Stochastic Processes in Physics and Chemistry*, Elsevier, Amsterdam (2007).
 - [22] M. O. Vlad et al., *Phys. Rev. E* **65**, 061110 (2002); M. O. Vlad et al., *Proc. Natl. Acad. Sci.* **13**, 10249-10253 (2004).
 - [23] O. Hallatschek, P. Hersen, S. Ramanathan, and D. R. Nelson, *Proc. Natl. Acad. Sci.* **104**, 19926-19930 (2007).
 - [24] J. Männik et al. *Proc. Natl. Acad. Sci.* **35**, 14861-14866 (2009).
 - [25] P. B. Raney and M. Travisano *Nature* **294**, 69-72 (1998).